remote sensing

MDPI

Article

Spatial–Temporal Changes in Land Use and Their Driving Forces in the Circum-Bohai Coastal Zone of China from 2000 to 2020

Jian Cui [1], Wenxin Ji [1], Peng Wang [2], Mingshui Zhu [2] and Yaohui Liu [1,*]

[1] School of Surveying and Geo-Informatics, Shandong Jianzhu University, Jinan 250101, China
[2] Ji'nan Institute of Survey and Investigation, Jinan 250101, China
* Correspondence: liuyaohui20@sdjzu.edu.cn

Abstract: Over the past two decades, the location and morphology of the coastline, as well as the land use/land cover (LULC) in the Circum-Bohai region in China, have undergone significant changes due to rapid industrialization and urbanization. Analyzing the temporal and spatial variation in coastal lines and LULC can provide a meaningful basis for the rational allocation of land resources. Using Landsat TM/OLI series dates from the Google Earth Engine (GEE) platform, this study applied the Linear Superposition Water Index (LSWI) and the Otsu threshold method (OTSU) algorithm to extract and analyze the coastline of the Circum-Bohai region. Additionally, the Random Forests (RF) method was employed to extract LULC information in the coastal zone. Using the geographical detector, we further explored the influence of social and economic factors, as well as natural factors, on spatial differentiation mechanisms of LULC change in the Circum-Bohai. Our results show that between 2000 and 2020, the Circum-Bohai coastline generally expanded towards the ocean by a total of 1062.99 km. The highest rate of change occurred during 2010 to 2015, and human activities were the primary cause of most of the changes, with the exception of the Yellow River Delta, where natural factors were dominant. The main types of LULC in the study area from 2000 to 2020 were farmland and construction land. The area of farmland proportion decreased by 1.75%, while the area of construction land proportion increased from 16.73% to 29.54%. Our findings indicate that the degree of land use in the Circum-Bohai is deepening. Based on our factor detection analysis, the added value of the secondary industry was the most critical influencing factor on LULC. Furthermore, the combined effect of the added value of the secondary industry and gross domestic product (GDP) has a significant driving impact on LULC. These findings can provide reference and data support for the sustainable development and comprehensive management of land resources. The relevant departments can use these results to prompt corresponding policies for the rational allocation of land resources.

Keywords: Google Earth Engine (GEE); Circum-Bohai coastal zone; Linear Superposition Water Index (LSWI); Random Forests (RF); geographical detector; driving force

check for updates

Citation: Cui, J.; Ji, W.; Wang, P.; Zhu, M.; Liu, Y. Spatial–Temporal Changes in Land Use and Their Driving Forces in the Circum-Bohai Coastal Zone of China from 2000 to 2020. *Remote Sens.* **2023**, *15*, 2372. https://doi.org/10.3390/rs15092372

Academic Editor: Georgios Mallinis

Received: 9 March 2023
Revised: 19 April 2023
Accepted: 27 April 2023
Published: 30 April 2023

1. Introduction

Affected by the rapid improvement of the world's economy and the extensive comprehensive impact of human and marine activities, global coastlines have undergone varying degrees of change, and the land use degree (LUD) in the coastal zones has also continued to deepen. Countries worldwide have increasingly prioritized the development, utilization, and conservation of their marine resources [1]. Monitoring the spatial and temporal changes in coastline morphology and coastal zone land use/land cover (LULC) is crucial for regional social and economic development, resource environment balance, and promoting sustainable economic development in coastal areas [2].

With the increase in the number of remote sensing satellites and the improvement of image resolution [3–5], advanced remote sensing technology and multi-spatial resolution remote sensing image data have gradually provided reliable technical means and data support for monitoring coastline change and coastal land use/land cover change (LUCC). The selection and application of the coastline extraction method is the key aspect in the process of monitoring coastline change using remote sensing technology [6]. Relevant studies have employed various methods to extract and analyze different types of coastlines at various scales in different regions based on multi-source multi-spatial resolution remote sensing image data, including visual interpretation [7], Normalized Difference Water Index (NDWI) [8], Tasseled Cap Transformation (TCT) [9], Automated Water Extraction Index (AWEI) [10], automated edge detection algorithms [11], Support Vector Machine (SVM), Maximum Likelihood (ML) [12], Modified Normalized Difference Water Index (MNDWI) [13], active connection matrix (ACM) [14], convolutional neural network (CNN) [15], and others. Particularly, the water index method is usually employed for research on large-scale and long-term monitoring of coastal changes. The NDWI, TCT, and MNDWI are the most commonly used methods [16]. Since the Otsu threshold method (OTSU) [17] is very suitable for cases where the gray values of the segmentation target and the segmentation background are significantly different [18], it is often integrated with NDWI, TCT, MNDWI, and other water index algorithms to extract large-scale coastlines.

In previous studies on LUCC monitoring in coastal zones, the acquisition of LULC information can be categorized into two general types. The first method is mainly to obtain LULC information in the study area through relevant datasets [19]. Based on different LULC classification datasets, researchers have analyzed and studied the land use of coastal zones [20,21]. The second method involves using supervised or semi-supervised classification methods to classify coastal zone LULC and then obtain coastal LULC information. Due to the superior classification effect and experimental accuracy, the Random Forest (RF) [22] algorithm is often used in the LULC information classification and extraction task [23]. Researchers usually employ the RF classification model to classify the LULC information [24], and other methods are combined to investigate and analyze its spatial and temporal evolution [25,26]. The selection of LULC research areas also has its own characteristics, including inland areas [23], river coasts [27], and coastal areas [26,28]. Exploring the driving factors that affect LUCC is helpful to further analyze the LUCC model in the Circum-Bohai region, which is of great significance for natural resources management. At present, qualitative or quantitative methods are usually utilized to determine the driving factors affecting a specific change [27]. Among them, qualitative analysis can only characterize the influence of various impact factors and cannot quantitatively analyze their effect. Moreover, it often ignores the spatial relationship between the change and the influencing factors. Geodetector is a method that can detect a certain geographical phenomenon or a certain spatial variation and reveal the driving factors behind it [23,27]. It has been widely used in vegetation coverage change [29], LUCC [23,27], ecological environment vulnerability [30], and so on.

In remote-sensing-technology-based research and remote sensing image analysis, the screening and processing of massive remote sensing data are crucial. However, in previous related research, difficulties in data acquisition and processing and low interpretation efficiency have often been observed [31]. To solve these problems, the emergence of Google Earth Engine (GEE) [27] provides new ideas and methods for massive data processing in large-scale and long-term research projects [27]. The GEE platform has the capability to process data in batches rapidly, regardless of temporal and spatial limitations. [31]. Using the GEE platform, relevant studies have realized the extraction of crop area [32], surface water changes [33], ecological environment quality evaluation [34,35], and LUCC [36,37]. These studies have fully verified the feasibility and effectiveness of the GEE platform in downloading, processing, and computing data. Therefore, we can efficiently research coastline spatial–temporal variation and coastal LUCC monitoring using the GEE platform. However, in related research, coastlines are often extracted using a single method, and coastal LUCC information extraction is typically focused on large-scale areas. Furthermore, there are computational complexities in exploring the driving factors behind coastal LUCC.

As one of the areas most affected by human activities in China, the Bohai Sea occupies an important position in the development of national economic strategy [38]. However, with the human activities and deepening of land development and utilization in the Circum-Bohai coastal area, artificial breeding and port construction have caused spatial differences in LULC in the coastline and coastal zone over time, which pose challenges to the protection and development of the marine and land ecological environment in the Circum-Bohai area. Therefore, it is essential to explore the changes in the Circum-Bohai coastlines, as well as to explore the spatial pattern of LULC and the driving factors behind LUCC in the Circum-Bohai coastal area. Hence, investigating alterations in the Bohai Sea coastline and analyzing variations in the LULC spatial model are imperative to comprehend the key driving factors.

In this study, we aim to explore the process of coastline changes and coastal LUCC in the Circum-Bohai coastal area from 2000 to 2020 using the Landsat TM/OLI series data on the GEE platform. First, the coastline of the Circum-Bohai area was extracted through the linear fusion of TCT and MNDWI combined with the OTSU method. Then, we explored the spatial and temporal pattern change in LULC information in the Circum-Bohai coastal area based on the RF classification method. Lastly, the transfer matrix and driving factors behind the changes in the LUD are discussed using the Geodetector model.

The remainder of this study is organized as follows: Section 2 presents the study area and data. Section 3 describes the methods used in this study. Section 4 presents the experimental results. The discussion and conclusion are presented in Sections 5 and 6, respectively.

2. Study Area and Data

2.1. Study Area

The study area is situated in the eastern part of China, stretching from Dalian City in the Liaodong Peninsula to Yantai City in the Shandong Peninsula, spanning from 117°26′58″E to 122°23′47″E and 36°59′22″N to 41°0′34″N. Additionally, the Bohai Sea is the only inner sea in China [28]. The study area covers 13 cities (presented in Figure 1). Within the Bohai Bay region, there are three predominant bays: Bohai Bay, Liaodong Bay, and Laizhou Bay. Among them, Pulandian Bay area (A) in Dalian is one of the key areas of coastline change in the Circum-Bohai. Liaodong Bay Area and Laizhou Bay area contain two large estuary deltas, Liaohe River Delta (B) and Yellow River Delta (D), respectively, which are two important wetland nature reserves in China [39]. Additionally, Tangshan Port Area (C) in Tangshan City, Bohai Bay area, features significant artificial land [40].

Due to the uniqueness of the geographical conditions and the complexity of economic development in the Circum-Bohai, this study utilized the land-side buffers along the coastline to define the regional scope of LUCC research in the area to more accurately and intuitively express the LUCC in the Circum-Bohai. Specifically, the coastline was extracted every five years from 2000 to 2020 in the Circum-Bohai region, and a unilateral buffer with a radius of 10 km was created on the land side along the coastline [41]. Five buffers were then obtained and synthesized to derive the LUCC results in the Circum-Bohai coastal zone.

2.2. Data

The study employed Landsat TM/OLI series data from 2000 to 2020 obtained from the GEE platform. A total of 1533 remote sensing image data were used in the coastline extraction experiment on the Circum-Bohai, including data from 2000, 2005, 2010, 2015, and 2020. For the 2000, 2010, and 2020 coastal land use and land cover (LULC) classification, a total of 1130 scene images data were utilized. The remote sensing image data underwent several preprocessing stages such as filtering, cloud removal, splicing, cropping, masking, and more. The data sources are provided in Table 1.

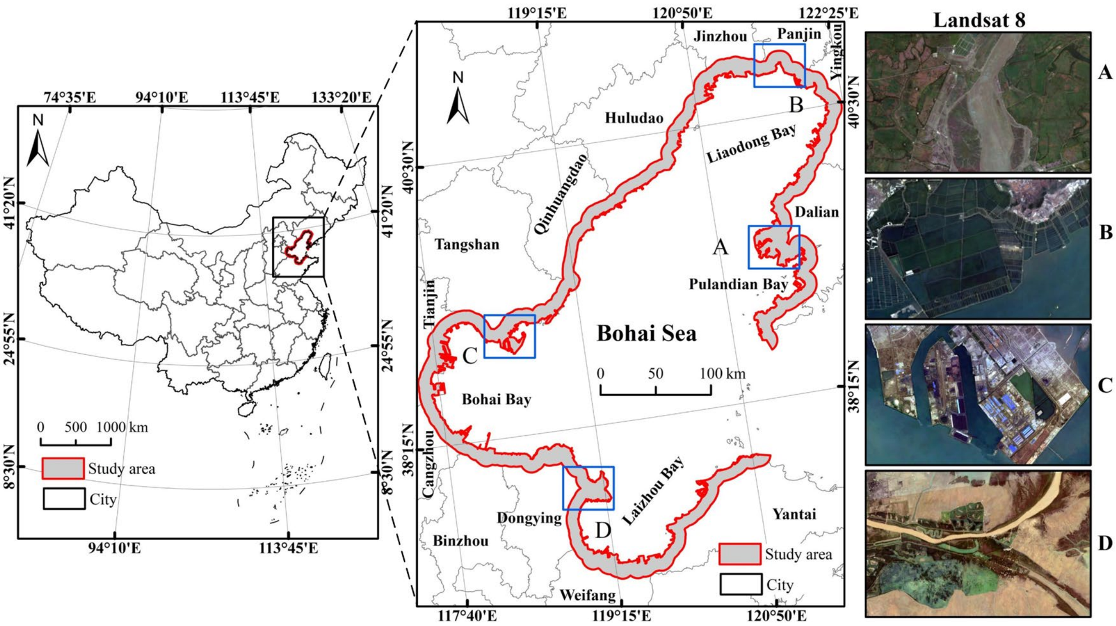

Figure 1. Study area: (**A**) Pulandian Bay area; (**B**) Liaohe River Delta; (**C**) Tangshan Port; (**D**) Yellow River Delta.

Table 1. Data sources.

Sensor	Spatial Resolution(m)	Year	Band Used
Landsat-5 TM	30	2000, 2005, 2010	Blue, Green, Red
Landsat-8 OLI	30	2015, 2020	NIR, SWIR

Considering the unique geographical conditions of the Circum-Bohai coastal zone, such as the frequent occurrence of two estuary deltas and reclamation, we divided the LULC types into eight categories according to the actual situation of the study area, namely, farmland, grassland, forest land, construction land (urban, residential area, traffic land, and industrial land), waterbody (seawater and inland freshwater), unused land (sand and bare land), natural wetland (beach and wetland), and artificial wetland (saltern, coastal reclamation, and artificial breeding). The RF classification method was then employed to classify the LULC of the Circum-Bohai coastal zone [42].

To better distinguish the various categories in the study area, this study comprehensively considered and calculated the normalized difference vegetation index (NDVI), normalized difference build and soil index (NDBI), enhanced vegetation index (EVI), NDWI, and MNDWI, and constructed a classification feature set [27]. To construct a classification sample set, this study utilized high-resolution historical data from Google Earth Pro and performed visual interpretation. The sample points for the Circum-Bohai coastal zone in 2000, 2010, and 2020 were 1813, 1821, and 1828, respectively. To ensure the accuracy and reliability of the experiment, 70% of the samples from each period were used to establish the training sample, while 30% of the samples were utilized to establish the verification sample [43].

The geographic detector model was utilized to explore the internal driving mechanisms of LUCC in the study area by analyzing both socioeconomic and natural aspects [25]. Relevant information on some of the impact factors was obtained from the Chinese Academy of Sciences (https://www.resdc.cn/ (accessed on 10 February 2023)) [27], including population density (X1), gross domestic product (GDP) (X2), annual average precipitation (X8), annual average temperature (X9), slope (X10), aspect (X11), and elevation (X12). At the same time, the other part used the statistical yearbooks of the provinces and cities in the study area to collect data on the secondary industry added value (X3), tertiary industry added value (X4), urbanization rate (X5), the total value of fishery production (X6), and port throughput (X7) [27]. The information on influencing factors is shown in Table 2.

Table 2. Influencing factors in this study.

Type	Influencing Factors	Index	Unit
Socioeconomic factor	X1	population density	Ten thousand people/km^2
	X2	gross domestic product	billion CNY
	X3	secondary industry added value	million CNY
	X4	tertiary industry added value	million CNY
	X5	urbanization rate	%
	X6	total fishery output	million tons
	X7	port throughput	million tons
Physical factor	X8	annual average precipitation	mm
	X9	annual average temperature	°C
	X10	slope	/
	X11	aspect	°
	X12	elevation	m

3. Methodology

The Landsat TM/OLI series data after preprocessing in the experimental year were selected from the GEE platform, and utilized the linear fusion TCT, MNDWI method, and OTSU algorithm to extract and analyze the changes in the Circum-Bohai coastline. The RF classification was employed to classify the LULC types in the study area, while the land use transfer matrix was utilized to explore LULC type transfers. Additionally, the land use degree index (LUDI) was calculated to evaluate the change in land use. To explore the mechanisms of socioeconomic and natural factors influencing LUCC, factor detection and interaction detector in Geodetector were used for analysis. The experimental workflow is depicted in Figure 2.

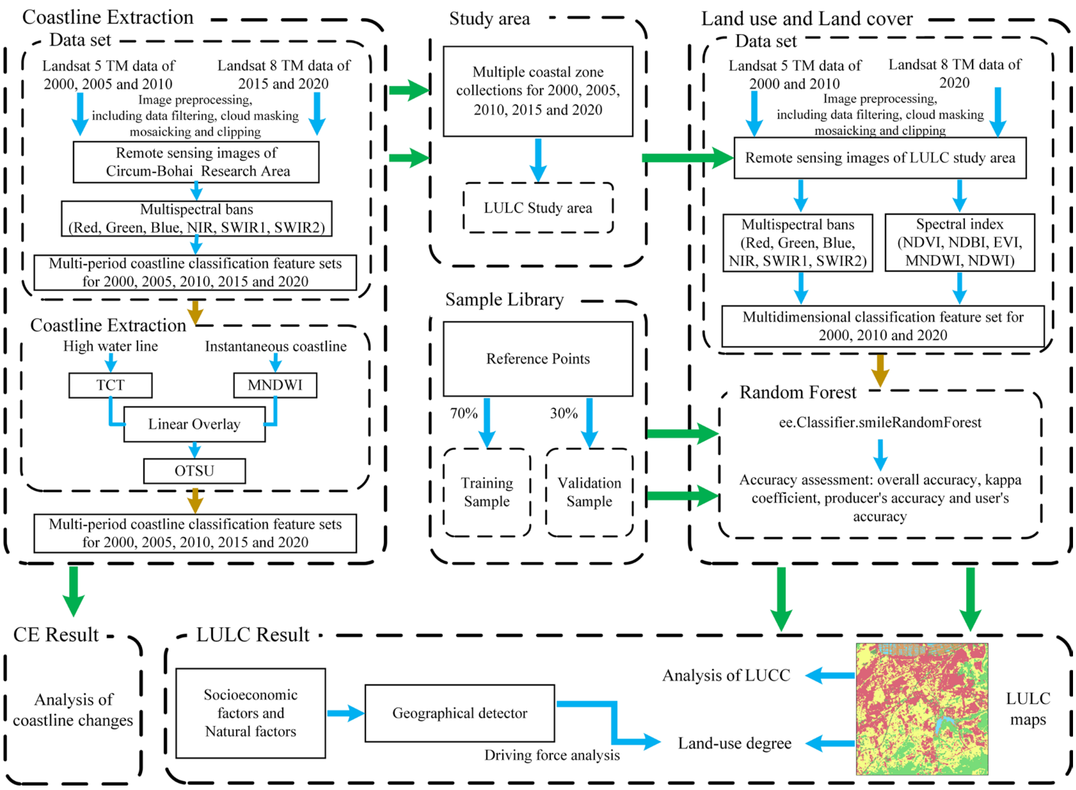

Figure 2. The flowchart of this study.

3.1. Long Time-Series Coastline Extraction Method

3.1.1. Water Index Method

Landsat TM/OLI series data in the GEE platform were utilized to accurately differentiate water and land in the Circum-Bohai by linearly fusing TCT [9] and MNDWI [13]. Specifically, TCT and MNDWI were used to calculate the remote sensing data for five periods from 2000 to 2020. Two gray image data of each period were obtained, and each pixel was linearly superimposed based on its gray value to synthesize gray image data. Finally, five years of gray images with varying gray values were generated to reflect water and land. This method is named the Linear Superposition Water Index (LSWI) for ease of reference. The mathematical expression for TCT is as follows:

$$\mu = R_X^T + r \tag{1}$$

where R is the tasseled cap transformation coefficient; X is the pixel value of different bands; r is the constant offset; and μ is the gray value of each pixel in different bands after tasseled cap transformation [44].

MNDWI mathematical is presented as follows:

$$MNDWI = (LG - LS)/(LG + LS) \tag{2}$$

where LG represents Green in Landsat TM/OLI series and LS represents SWIR/SWIR1 in Landsat TM/OLI series. $MNDWI$ is the gray value calculated for each pixel.

3.1.2. Otsu Threshold Method (OTSU)

The OTSU is an adaptive image segmentation algorithm based on the least square method [17]. Its principle is to calculate the segmentation threshold of the gray image by using the maximum inter-class variance and is therefore also called the maximum inter-class difference method [45]. OTSU possesses the characteristics of being unaffected by image brightness and contrast, along with fast segmentation speed and simple calculation.

The OTSU mathematical expression is as follows:

$$\sigma_B^2(t) = F_0(t)F_1(t)(\rho_0(t) - \rho_1(t))^2 \tag{3}$$

$$T = \arg \max_{0 \le t \le L-1} \sigma_B^2(t) \tag{4}$$

where $F_0(t)$ and $F_1(t)$ are the ratios of the pixels in the two regions; $\rho_0(t)$ and $\rho_1(t)$ are the pixel mean of the two regions, respectively. L represents the total gray level of the input image; T is the segmentation threshold obtained when $\sigma_B^2(t)$ reaches the maximum value [46].

3.2. Coastal Land Use Classification

3.2.1. Coastal LULC Classification and Its Accuracy Evaluation

The RF classification method commonly utilized in LULC information classification is a classification method based on the combination of classification decision trees [27]. Its basic units and principles are sets of decision trees and decision tree classifiers, respectively [47]. By utilizing each decision tree to perform multi-decision voting on the given samples for training and prediction, a classification selection can be obtained. This effectively improves the overfitting or underfitting problems that commonly arise in single decision trees [48]. The RF method possesses strong anti-interference performance, high classification accuracy, and classification efficiency [49]. In this study, the LULC is classified using the ee.Classifier.smileRandomForest (number of trees) function on the GEE platform. Experimental verification shows that when the number of decision trees is 500, the classification effect is comparatively precise, so 500 trees were then employed for RF classification [27].

The confusion matrix is a common method used to evaluate the accuracy of remote sensing classification results [50]. The accuracy of classification results is quantitatively analyzed by calculating user accuracy (UA), producer accuracy (PA), kappa coefficient (kappa), and overall accuracy (OA) based on the confusion matrix [23].

3.2.2. Land Use Degree Index

In this study, the LUDI is an indicator that reflects the degree of actual land use and development by humans. It is often utilized to explain the LUD and development [51]. The higher the value calculated by the grading index, the greater the level of land development and utilization in the region [23], and therefore the higher the degree of social and economic development in the area [52]. In order to analyze the LUD in the Circum-Bohai, the level of land development and utilization was evaluated using the LUDI. The calculation formula for l_a of the LUD is as follows:

$$l_\alpha = 100 \times \sum_{j=1}^{m} I_j \times P_j \tag{5}$$

where l_a is the calculated value representing the degree of land use, and its range is 100–400. I_j is a value representing the classification of different LUDI, P_j is the percentage of the j-th LUD classification area in the total area of the study area. According to the types of LULC and related research [25], this study divided the LULC into four different grades based on the land resource utilization degree and gives different classification indexes to each grade (presented in Table 3).

Table 3. Types and classification of LULC in the Circum-Bohai coastal zone.

Type	Uncultivated Land	Ecological Land	Agricultural Land	Construction Land
LULC types	Unused land (sand and bare land) Natural wetlands (beach, wetland)	Grassland Forest land Waterbody (seawater, inland freshwater)	Farmland Artificial wetland (saltern, coastal reclamation, artificial breeding)	Construction land (urban, residential area, traffic land, and industrial land)
Index of Classification	1	2	3	4

3.3. Geographic Detector

Geodetector [53] is a statistical technique for assessing the impact of selected variables on specific changes and identifying spatial changes. Geodetector includes factor detection, interactive detection, ecological detection, and risk detection [54]. This study mainly used factor detection and interactive detection in geographic detectors, which can explore the spatial divergence interpretation of each influencing factor alone or after interaction [27]. Specifically, LUDI is used as Y, the impact factor is used as X, and the decisive index q is introduced to evaluate each impact factor. The geographic detector model is presented as follows:

$$q = 1 - \frac{\sum_{h=1}^{L} N_h \sigma_h^2}{N\sigma^2} \tag{6}$$

$$W_h = \sum_{h=1}^{L} N_h \sigma_h^2 \tag{7}$$

$$T_h = N\sigma^2 \tag{8}$$

where $h = 1, \ldots, L$ is the strata of variable Y or factor X. N_h are the number of elements in the layer and N is the whole region. σ_h^2 and σ^2 are the variances in the Y values in the layer h and the whole region, respectively. W_h and T_h are within the sum of squares and the total sum of squares, respectively. The range of q is [0, 1]; the larger the value is, the more obvious the spatial differentiation of Y is.

4. Results

4.1. Coastline Change Analysis

4.1.1. Validation of Coastline Extraction Method

To validate the accuracy of coastline extraction, we utilized four methods, namely NDWI, TCT, MNDWI, and LSWI, to distinguish between sea and land in three different areas: A, B, and C, in the year 2010. These areas represent different shoreline types, including natural (A), artificial (B), and beach (C), which are affected by diverse factors such as human activities and natural processes. The experimental results of coastline extraction by the four methods are shown in Figure 3.

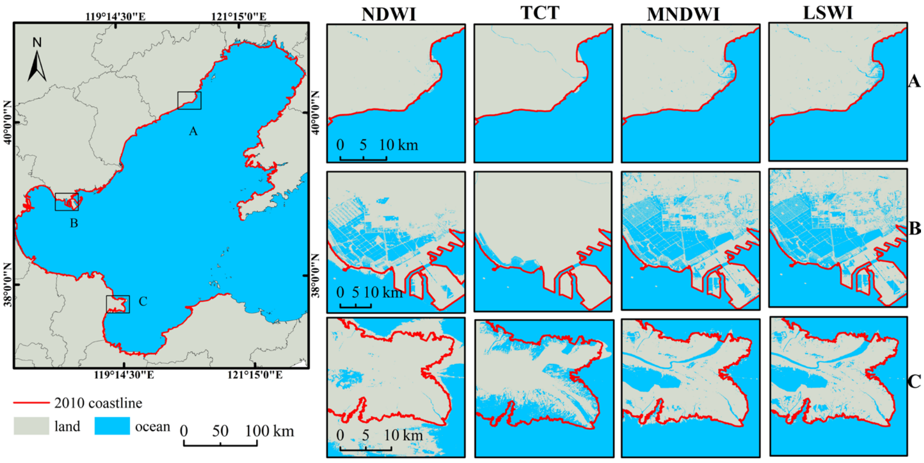

Figure 3. Three typical areas (**A**–**C**) and their classification results: (**A**) is part of the coastline of Huludao City; (**B**) is Tangshan Port; (**C**) is the Yellow River Delta.

The four methods were evaluated based on their effectiveness in segmenting water and land in each area. The results show that the segmentation effects of all four methods are good in the natural shoreline area (A). In the artificial shoreline area (B), only the MNDWI and LSWI methods produced better results. In the beach shoreline area (C), the LSWI method outperformed the other methods. Therefore, the LSWI water extraction method was selected for the segmentation of waterbodies in the Circum-Bohai coastal in this study, as it provides a better sea–land segmentation effect.

In summary, the LSWI method was found to be the most effective for distinguishing between sea and land, particularly in areas that are strongly influenced by natural or human factors. This method was thus selected to extract waterbodies and segment the ocean and land, ensuring the accuracy of the study's results.

4.1.2. Coastline Change Analysis

Figure 4 displays the extraction results of coastline length change in the Circum-Bohai from 2000 to 2020. It demonstrates that the coastline length fluctuation in the Circum-Bohai region has generally increased over the past 20 years, with a total increase of 1062.99 km. Specifically, the coastline of the Circum-Bohai region exhibited a slight upward trend from 2000 to 2005, increasing by 194.1 km. From 2005 to 2015, the coastline length of the Circum-Bohai gradually increased, and the rate of change accelerated, with a total increase of 1087.9 km during this period. Finally, from 2015 to 2020, the coastline length decreased by 24.91 km.

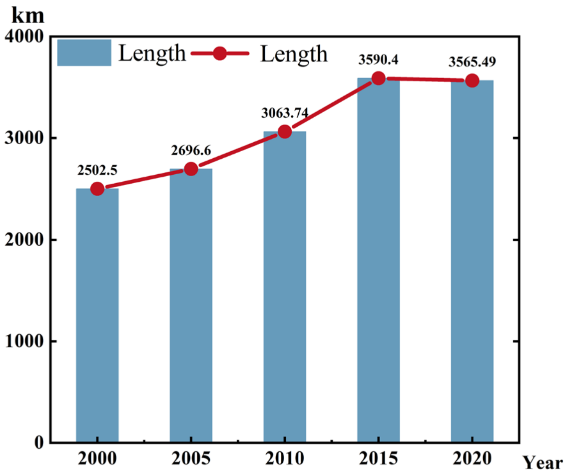

Figure 4. Length changes of Circum-Bohai coastline from 2000 to 2020.

Comparing the coastline change results obtained by the LSWI method with the classified images, it can be seen that the primary change areas of the Circum-Bohai coastline are Laizhou Bay, Bohai Bay, and Liaodong Bay. Among them, the artificial aquaculture and salt field construction in Liaodong Bay and Laizhou Bay are more prominent, and the changes in the Circum-Bohai from 2000 to 2020 are more significant. The most significant changes in the region are mainly distributed in the Bohai Bay artificial reclamation, wharf construction, and other related areas, particularly in Tianjin and Tangshan. These changes are also related to urban development policy directives and the rapid development trend of the maritime economy. Unlike these reasons, the changes in the Yellow River Delta's coastline are due to natural factors, as the coastline type of the Yellow River Delta is mainly a tidal flat coast formed by sediment accumulation brought by the Yellow River. From 2000 to 2020, the Yellow River Delta's location changed, leading to significant changes in the coastline's position in the region. In addition to the above areas, the coastline changes in other areas are relatively small because the coastlines of these regions are mostly natural and have not been extensively developed and utilized.

Figure 5 illustrates the overall changes in the coastline, with typical change areas a and b representing the artificial coastline, while c represents the natural coastline. Among them, a is the artificial breeding area, b is the Huanghua Port, and c is the Yellow River Delta. The analysis of the Circum-Bohai coastline changes revealed that the majority of changes occurred in regions where human activities, such as artificial aquaculture, artificial land, and wharves, were prevalent, while changes in the Yellow River Delta are due to natural factors. Limited coastline changes in other areas are attributed to their relatively natural state. This study provides vital insights into the complex interplay between natural and human factors contributing to changes in coastal environments.

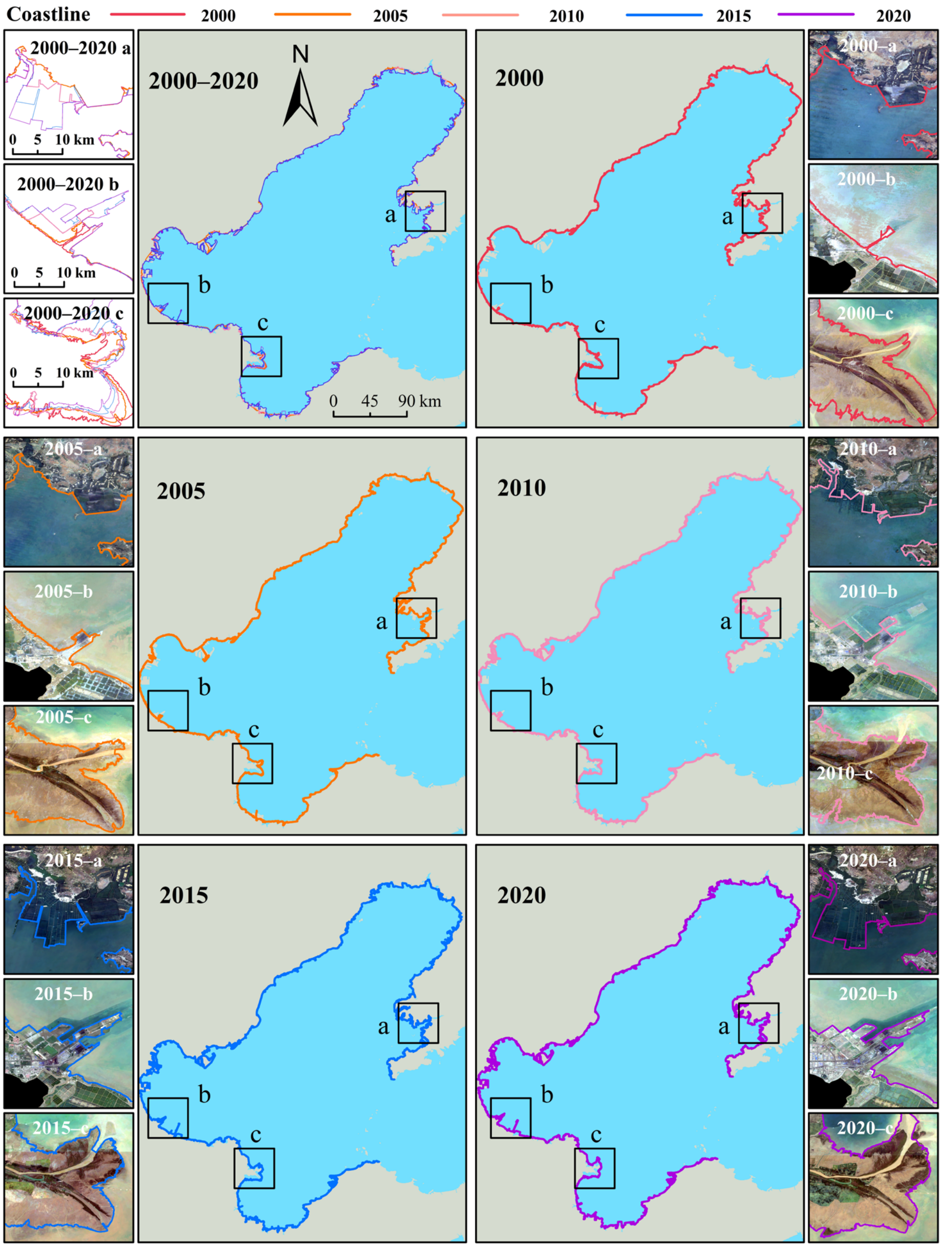

Figure 5. The changes of coastlines in the Circum-Bohai region from 2000 to 2020, where a and b are artificial coastlines and c is the natural coastline. (**a**) Pulandian Bay area; (**b**) Huanghua Port; (**c**) Yellow River Delta.

4.2. Long Time-Series LUCC Analysis of Coastal Zone

4.2.1. Accuracy Evaluation

The accuracy of LULC information classification in LUCC analysis is essential for further research. In this study, the confusion matrix was employed to evaluate the accuracy of LULC classification results in the Circum-Bohai region in 2000, 2010, and 2020. The results of the LULC classification accuracy evaluation are presented in Table 4. The OA for 2000, 2010, and 2020 was 91.15%, 88.54%, and 92.08%, respectively. Meanwhile, the kappa was 0.89, 0.86, and 0.90, respectively. The classification results of OA and kappa for each period were above 85%, which indicates high classification accuracy for different LULC types. Therefore, the classification achieved an acceptable level of accuracy, indicating that the results are both reasonable and reliable.

Table 4. Accuracy evaluation.

LUCC Types	2000		2010		2020	
	P_{UA} (%)	P_{PA} (%)	P_{UA} (%)	P_{PA} (%)	P_{UA} (%)	P_{PA} (%)
Farmland	88.42	94.28	87.76	93.93	89.57	94.5
Forest land	90.63	93.55	92.3	93.98	91.72	92.36
Grassland	100	50	100	72.73	100	25
Waterbody	96.95	92.03	86.25	92.62	87.5	90.51
Construction land	90.77	91.47	89.34	90.76	94.72	96.34
Unused land	85.71	88.24	90	46.15	100	60.71
Natural wetlands	90.09	86.96	71.19	79.25	91.04	88.41
Artificial wetland	94.06	90.91	90.86	82.87	93.13	91.35
P_{OA} (%)	91.15		88.54		92.08	
Kappa coefficient	0.89		0.86		0.90	

4.2.2. LULC Change Analysis

In the long-term LUCC analysis of the coastal zone between 2000 and 2020, the proportion and distribution of LULC in the 10 km buffer of the coastal zone of the Circum-Bohai have changed significantly. Figure 6 shows that this area's dominant LULC types are primarily farmland and construction land. The area of farmland decreased slightly from 31.23% to 29.48% from 2000 to 2020. In contrast, construction land improved from 16.73% to 29.54%, with an overall increase of 2289.84 km^2. Constructed wetland areas accounted for approximately 22% during 2000 to 2020, and the overall change was not significant. However, natural wetlands experienced a decreasing tendency, in 2020 the area accounted for around 10%. The proportion of forest land and waterbodies showed a decreasing trend. The main reason for this is that the continuous expansion of construction land between 2000 and 2020 encroached on the distribution areas of other LULC categories.

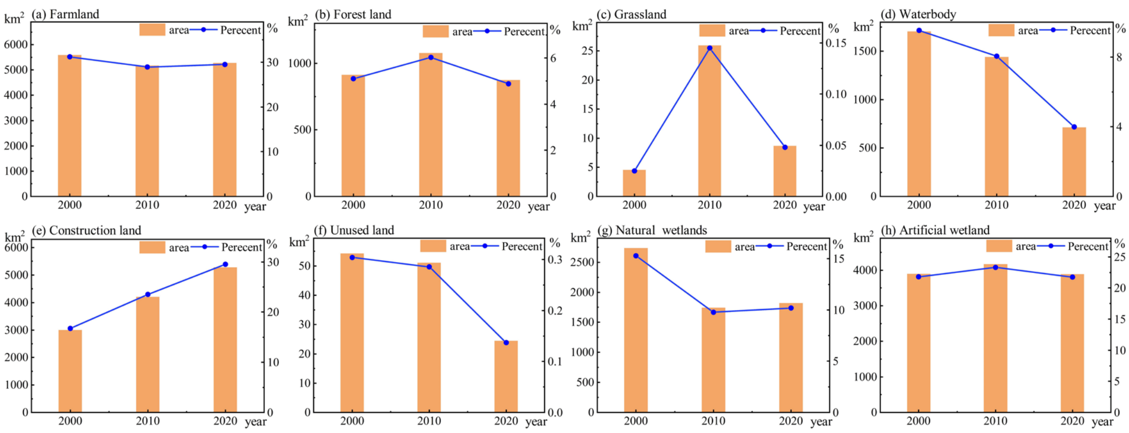

Figure 6. The proportion of LULC types changed from 2000 to 2020.

The LULC distribution of each category in the study area is shown in Figure 7; farmland is primarily found in the coastal zones of Yantai City in Shandong Province, Qinhuangdao City in Hebei Province, Huludao City, and Dalian City in Liaoning Province, which the primary industry economy has a relatively high proportion. The distribution of construction land is more dispersed, with concentrations in the economically developed and mature marine transport industry of the Tianjin and Tangshan coastal zones, e.g., the b in Figure 7 is Tianjin Port. Artificial wetlands are mainly distributed in the northeast of Laizhou Bay, Bohai Bay, and Liaodong Bay, where artificial breeding and reclamation are vigorously developed. Water is mainly distributed in rivers, lakes, and buffer zone at both ends of the sea. Natural wetlands are primarily located in the Liaohe River Delta (a) and Yellow River Delta (c).

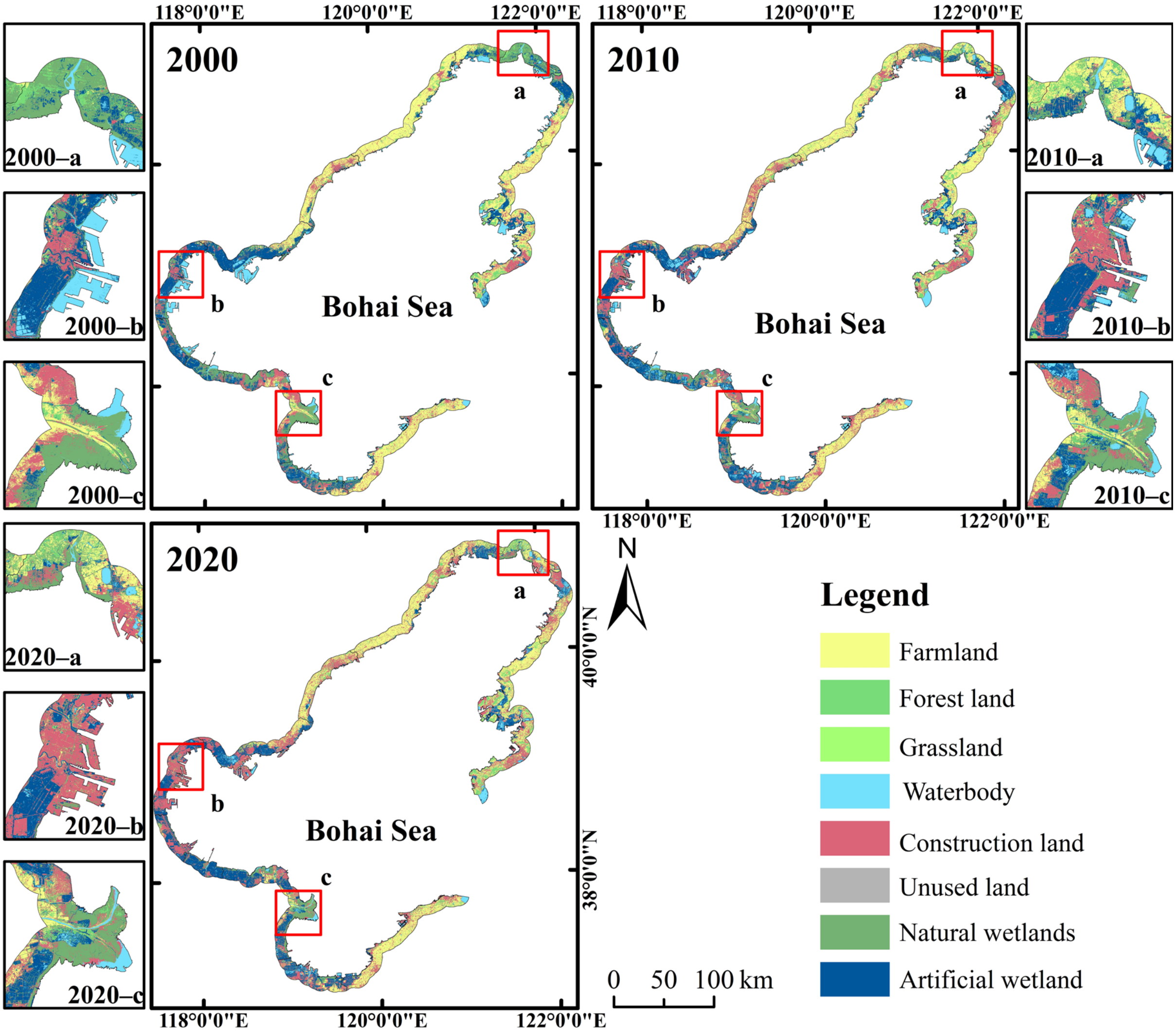

Figure 7. Spatial distribution of LULC in the Circum-Bohai from 2000 to 2020: (**a**) Liaohe River Delta; (**b**) Tianjin Port; (**c**) Yellow River Delta.

4.2.3. LULC Spatiotemporal Change Analysis

To provide a clear representation of the transfer relationship between the LULC types, we employed the transfer matrix to further analyze the transformation of LULC types from 2000 to 2010, 2010 to 2020, and 2000 to 2020, as shown in Figure 8. Overall, the construction land area has increased significantly, while the areas of waterbodies and natural wetlands have decreased significantly. The farmland area has decreased slightly, while the areas of forest land and artificial wetlands remained unchanged. Figure 8a shows that from 2000 to 2010, the construction land area increased rapidly, and the natural wetlands area showed a downward trend, mainly converted into artificial wetlands. Forests increased slightly, mainly from cropland. Figure 8b shows that from 2010 to 2020, the area of construction land increased, mainly at the expense of constructed wetlands. The water area decreased, mainly being transferred to artificial wetlands, and the forest land area was reduced due to the conversion of a small amount of forest land into farmland. Figure 8c illustrates the main transformation of LULC types from 2000 to 2020, in which the construction land area is increasing, mainly from farmland, constructed wetlands, waterbodies, and natural wetlands. The areas of waterbodies and natural wetlands are decreasing. By contrast, the overall change in farmland, forest land, and artificial wetland areas is small.

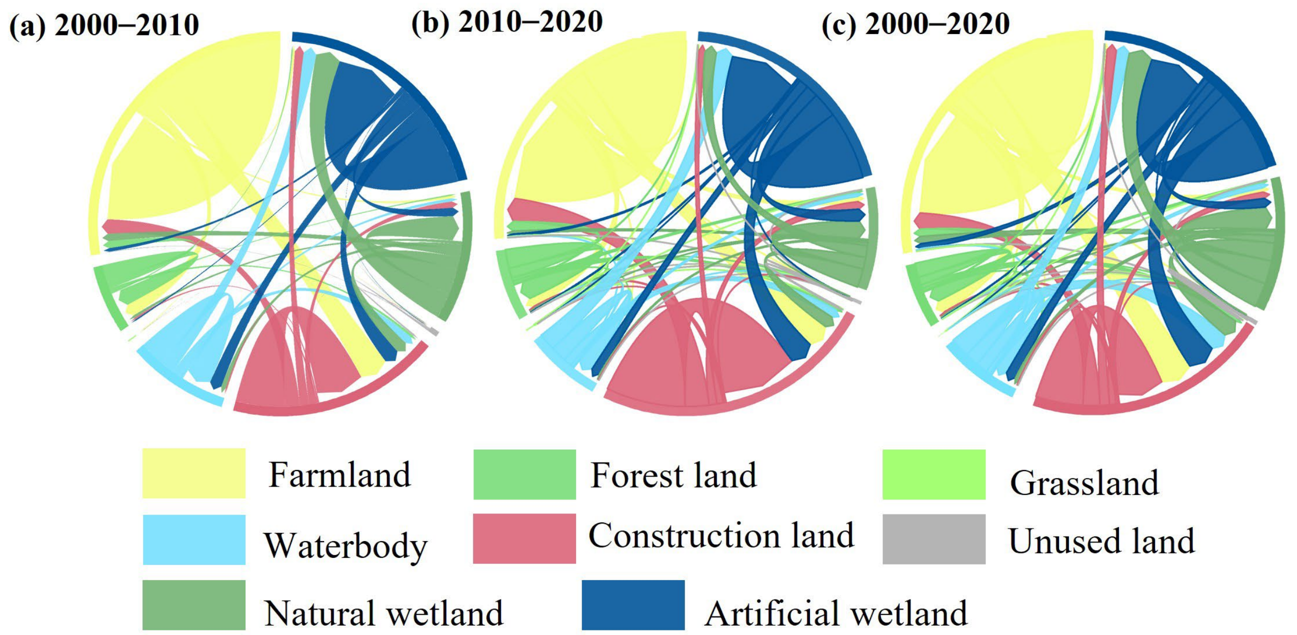

Figure 8. LULC type transfer of the Circum-Bohai coastal zone: (**a**) from 2000 to 2010; (**b**) from 2010 to 2020; (**c**) from 2000 to 2020.

4.2.4. Land Use Degree Index

The study area's comprehensive land use degree index was calculated based on the LULC classification results and used to classify different land types. The LUD spatial distribution map of the study area is displayed in Figure 9, utilizing a 1 km × 1 km grid for display. The findings reveal that LUD exhibits significant spatial differentiation, with the Bohai Bay area, which is significantly affected by human activities and economic development, having a much higher LUD than the Liaodong Bay and Laizhou Bay areas. This is likely due to the relatively developed urban economy in the Bohai Bay region, with construction land and artificial wetland being the dominant land types classified at a higher level of land use. In contrast, the Liaohe River Delta, a, and the Yellow River Delta, c, in Liaodong Bay and Laizhou Bay are dominated by natural wetlands, which experience fewer human disturbance activities leading to lower LUD. Additionally, there was an increasing trend observed in the degree of land use in coastal areas from 2000 to 2020, especially in region b in Figure 9, where LUD increased significantly.

4.3. Analysis of LUCC Driving Factors

Factor detection and interactive detection methods are commonly used to explore the impact of influencing factors on the spatial differentiation of LUD. Table 5 presents the *p*-values for the factor detection results from 2000 to 2020, which are all 0, indicating that the selected detection factors have a significant impact on the spatial heterogeneity of LUD. The q value in Table 5 represents the degree of spatial differentiation of the influencing factors on LUD in the study area. A higher value indicates a greater influence of the factor, or a stronger explanatory power of spatial differentiation.

As shown in Table 5, the added value of the secondary industry, urbanization rate, and population density between 2000 and 2020 are the key factors affecting LUD. However, over time, the q values of most influencing factors showed a downward trend, indicating that the driving effect of these factors gradually weakened.

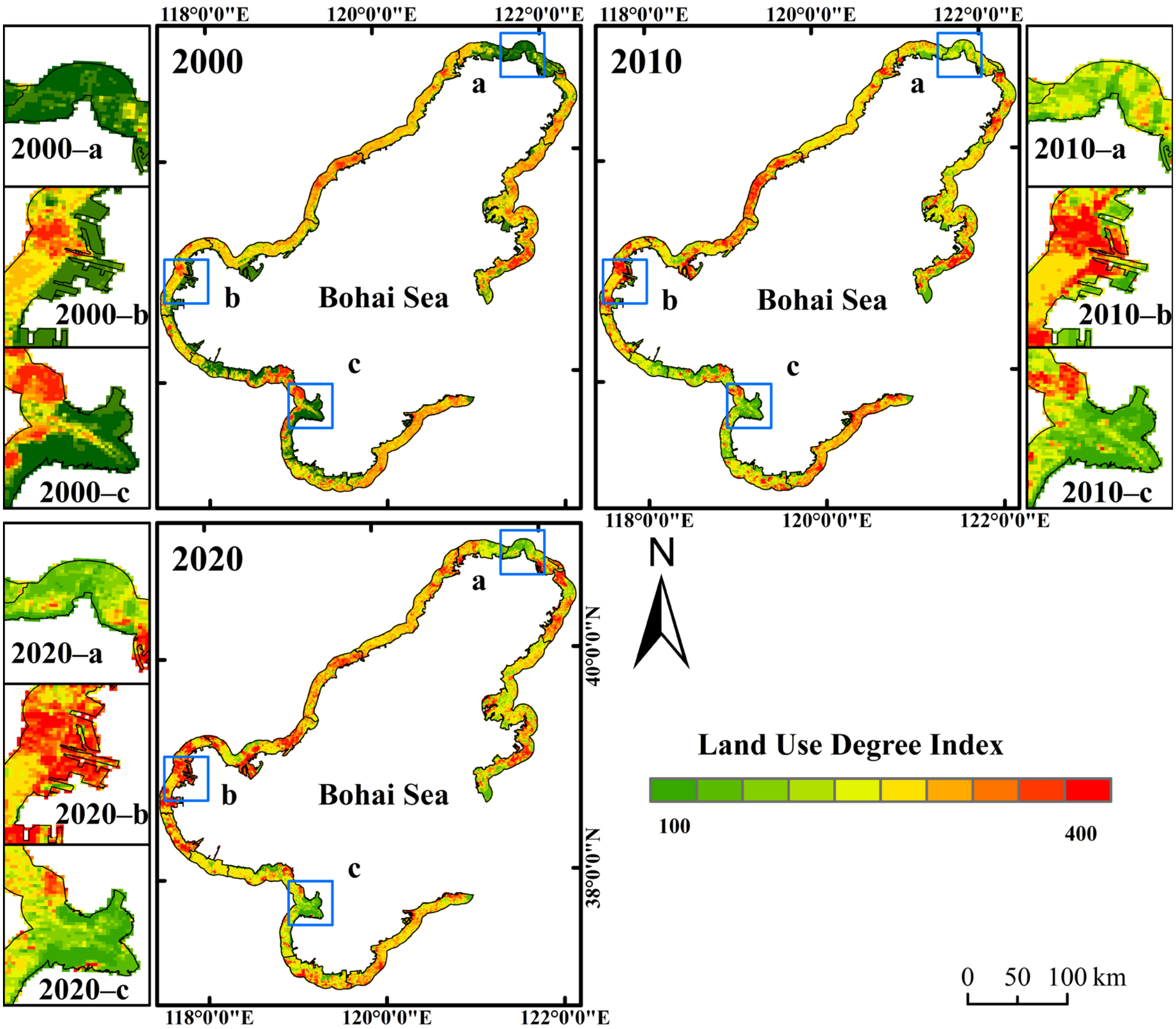

Figure 9. Spatial distribution of land use degree index in Circum-Bohai coastal zone from 2000 to 2020: (**a**) Liaohe River Delta; (**b**) Tianjin Port; (**c**) Yellow River Delta.

Table 5. Factor detection results.

Year		X1	X2	X3	X4	X5	X6	X7	X8	X9	X10	X11	X12
2000	q	0.12	0.13	0.08	0.18	0.08	0.19	0.06	0.06	0.11	0.04	0.01	0.04
	p	0	0	0	0	0	0	0	0	0	0	0	0
2010	q	0.09	0.09	0.10	0.07	0.11	0.03	0.12	0.05	0.01	0.04	0.09	0.09
	p	0	0	0	0	0	0	0	0	0	0	0	0
2020	q	0.06	0.06	0.10	0.07	0.09	0.05	0.05	0.05	0.01	0.05	0.06	0.06
	p	0	0	0	0	0	0	0	0	0	0	0	0

Unlike factor detection analysis, which examines the impact of single influencing factors on LUD in the study area, interactive detection investigates the effects of different influencing factors' interactions. As shown in Figure 10, the interaction between different influencing factors is more effective in explaining the spatial differences of LUD than a single factor, indicating that multiple factors affect the spatial heterogeneity of LUD in the study area. From 2000 to 2020, the interaction between GDP and the added value of the secondary industry, GDP and urbanization rate, GDP, and annual average precipitation effectively explained the spatial differentiation of land use in the region. The spatial differentiation characteristics of LULC in the Circum-Bohai region are mainly affected by the interaction of GDP, secondary industry added value, urbanization rate, and annual average precipitation. Although the average annual precipitation has a poor interpretation effect as a single factor, its impact on the spatial difference of LULC has been effectively demonstrated under the combined effects of GDP.

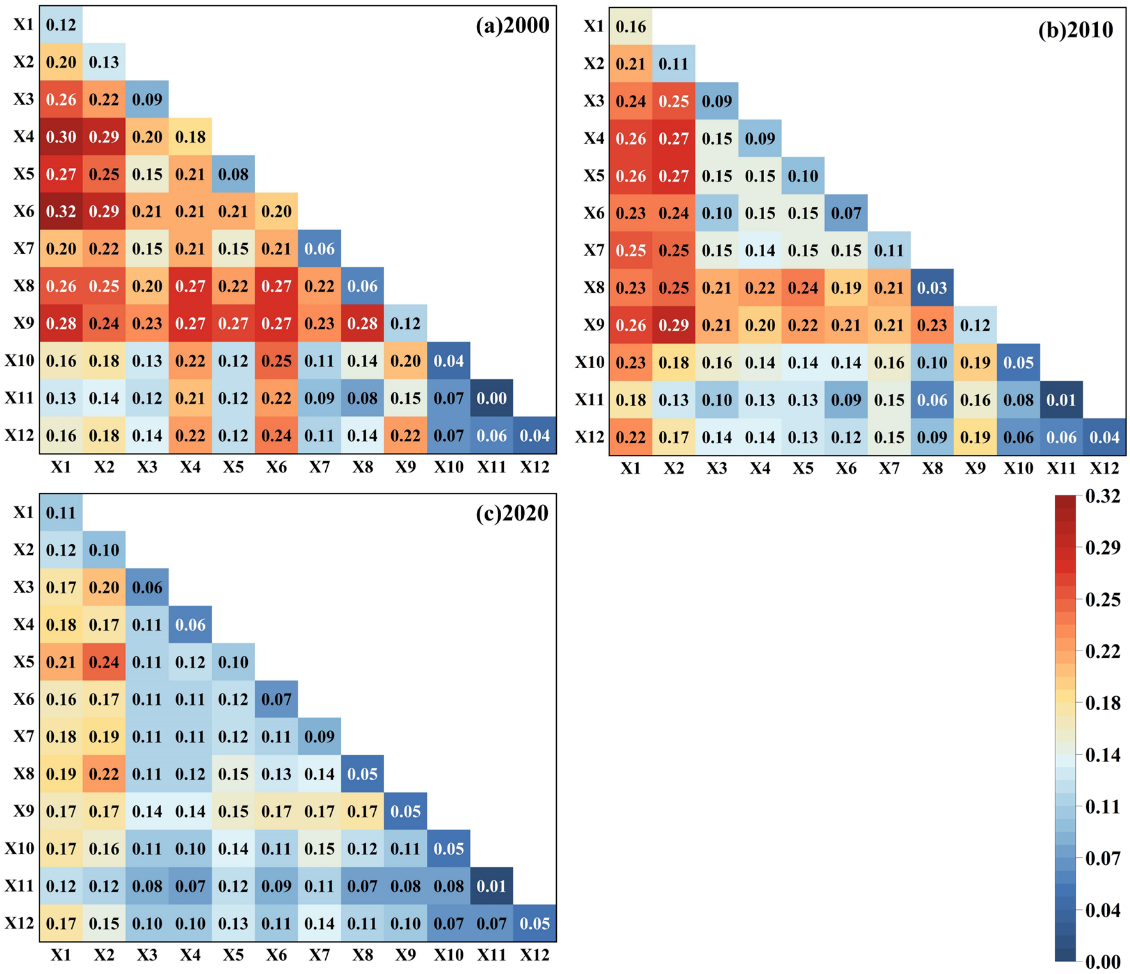

Figure 10. Interactive detection results.

5. Discussion

This study aimed to validate the effectiveness of several long-term and large-scale coastline extraction methods, such as NDWI, TCT, MNDWI, and LSWI. The results showed that the LSWI method is more effective in handling large differences between the TCT and MNDWI methods in certain areas. For instance, the TCT and MNDWI methods exhibited significant differences in artificial land, including ports, reclamation, and aquaculture, as well as the Yellow River Delta. By combining the gray values of the two exponential methods and using the OTSU method to reclassify marine land, these differences were effectively corrected, minimizing the likelihood of errors associated with using a single method. By fusing the regions with minor differences between these two methods, the classification achieved a clearer and more precise separation effect. As for morphological changes in the coastline position, the Dalian section, Bohai Bay area, and Laizhou Bay area in the Liaodong Bay region exhibited the most significant changes. This can be attributed to the deepening of China's development and utilization of marine resources, which led to the implementation of multiple coastal economic zones at the Circum-Bohai region in the early 2000s. The rate of coastline change was relatively slow from 2000 to 2005, significantly increased from 2005 to 2015, and decreased from 2015 to 2020. These changes can be attributed to China's successive policies aimed at constraining development and strengthening the protection of the Bohai Sea [55].

In the analysis of LUCC over the past two decades in the Circum-Bohai coastal zone, changes in the coastline from 2000 to 2020 were combined with a land-side buffer along the Circum-Bohai coastline. The results of LUCC were obtained through the employment of the RF classification algorithm, providing a more accurate and intuitive understanding of the region's LUCC. The coastal LUCC in the three-bay area was found to be significant, consistent with the observed changes in the coastline. This finding highlights the potential impact of coastline changes on the ecological benefits of the Circum-Bohai region and the adjacent coast's land use. Over time, there has been a gradual deepening of land use, in line with urban expansion and economic development. This trend is likely due to the increasing demand for land utilization and integration, leading to artificial breeding areas encroaching on wetland environments, and construction land encroaching on cultivated land and forest land [55].

In general, the coastal conditions of the Circum-Bohai region underwent significant changes between 2000 and 2020 due to human activities. Our findings revealed that urban expansion, artificial farming, and reclamation had not only impacted coastline changes but also influenced LUCC in the region. In other words, there is a correlation between LUCC and coastline change. Over the past two decades, changes in the location and morphology of the coastline and LUCC in the coastal zone of the Circum-Bohai region displayed pronounced spatial and temporal variations [28]. These variations were closely linked to the speed and level of regional development as well as local policies on marine development.

In regard to the LULC classification results, the OA and kappa obtained through the RF algorithm exceed the threshold of 85% recommended by the United States Geological Survey [23], with both metrics surpassing 86%. However, some errors were observed during the manual interpretation of certain areas. These errors may be attributed to the influence of image resolution and quality, as the spectral characteristics of water bodies and artificial aquaculture in some regions are similar, leading to the misclassification of these two categories. Manual visual interpretation and a comparison of various accuracy results indicated that the highest producer and user accuracies were achieved for forest land and construction land classification, suggesting that these two categories have more distinct spectral characteristics and are easier to classify.

During the computation process using GEE, computational limitations were encountered due to the large spatial span of the Circum-Bohai region and the significant number of required images for the experiment. Parallel experiments were necessary to relieve the computational pressure associated with issues such as calculation timeout, memory limit exceeding, and output errors. Future research should consider the use of higher-resolution remote sensing images, such as Sentinel-2 image data with a 10 m resolution, for LULC information extraction. Moreover, richer factors influencing LUCC should be employed for a more careful and comprehensive analysis of the driving factors impacting the coastal zone's LUCC situation.

6. Conclusions

This study aimed to explore the spatial and temporal evolution of coastline change and coastal zone LULC in the Circum-Bohai region of China from 2000 to 2020 and its driving forces. To achieve this, we first utilized the Landsat TM/OLI series data integrated in the GEE platform and employed the LSWI and the OTSU algorithm to extract the long time-series coastline of the Circum-Bohai. Furthermore, we analyzed and discussed the driving factors behind the LUCC in the study area using the geographic detector. The main findings can be summarized as follows:

(1) The length of the Circum-Bohai coastline underwent fluctuating changes from 2000 to 2020, displaying a phenomenon of initial increase followed by a decrease. The temporal changes of the coastline exhibited a slow–fast–slow trend, corresponding to periods of 2000 to 2005, 2005 to 2015, and 2015 to 2020. Spatially, there was a trend of land-to-sea expansion, with the change areas predominantly located in the three

major bay areas of Laizhou Bay, Bohai Bay, and Liaodong Bay. This change can be attributed to human activities as the main driving force.

(2) From 2000 to 2020, the types of LULC area are mainly farmland and construction land, followed by artificial wetlands and natural wetlands. The proportion of farmland and artificial wetland has remained unchanged, while the area of construction land has increased, and the natural wetlands and waterbodies have degraded. In terms of land type conversion, farmland and artificial wetland are primarily converted into construction land, while natural wetland is mainly converted into artificial wetland. From the perspective of land development, the utilization degree of Bohai Bay, Liaodong Bay, and Laizhou Bay is obviously higher than that of other regions, and it has gradually deepened over time.

(3) From 2000 to 2020, the added value of the secondary industry, urbanization rate, and population density were the single driving factors that significantly impacted the LUD in the study area. The interaction between GDP and the added value of the secondary industry has a significant impact on LULC change in the Circum-Bohai coastal zone.

The findings of this study would provide valuable data to support the management of land resources in the Circum-Bohai region and would assist relevant governments in formulating corresponding measures to achieve land and sea integration. Moreover, they would promote the scientific development of land and sea resources and improve the local eco-environment in the Circum-Bohai coastline area.

Author Contributions: Conceptualization, J.C. and W.J.; methodology, J.C.; software, W.J.; validation, J.C., M.Z. and P.W.; formal analysis, J.C.; investigation, M.Z.; resources, Y.L.; data curation, P.W.; writing—original draft preparation, W.J.; writing—review and editing, J.C.; visualization, W.J.; supervision, Y.L.; project administration, J.C.; funding acquisition, Y.L. All authors have read and agreed to the published version of the manuscript.

Funding: This research was jointly supported by the MOE Layout Foundation of Humanities and Social Sciences, grant number 17YJAZH013; the National Natural Science Foundation of China, grant number 42201077 and 42177453; and the Natural Science Foundation of Shandong Province, grant number ZR2021QD074.

Informed Consent Statement: Not applicable.

Data Availability Statement: Not applicable.

Conflicts of Interest: The authors declare no conflict of interest.

References

1. Uddin, K.; Khanal, N.; Chaudhary, S.; Maharjan, S.; Thapa, R.B. Coastal morphological changes: Assessing long-term ecological transformations across the northern Bay of Bengal. *Environ. Chall.* **2020**, *1*, 100001. [CrossRef]
2. Liu, Y.; Li, B.; Wang, Y.; Chen, L.; Li, X.; Hou, X. Evaluation of ecological connectivity in the coastal zone of Laizhou Bay-Yellow River Delta based on ecosystem service value. *Acta Ecol. Sin.* **2019**, *39*, 7514–7524. [CrossRef]
3. Cui, J.; Zhu, M.; Mi, H.; Liu, Y. Evaluation of Eco-Environmental Quality and Analysis on Spatio-Temporal Variation in Jinan, China. *Pol. J. Environ. Stud.* **2022**, *31*, 1061–1072. [CrossRef] [PubMed]
4. Yang, X.; Meng, F.; Fu, P.; Zhang, J.; Liu, Y. Instability of remote sensing ecological index and its optimisation for time frequency and scale. *Ecol. Inform.* **2022**, *72*, 101870. [CrossRef]
5. Kang, Y.; Meng, Q.; Liu, M.; Zou, Y.; Wang, X. Crop classification based on red edge features analysis of GF-6 WFV data. *Sensors* **2021**, *21*, 4328. [CrossRef]
6. Wu, Y.; Liu, Z. Research progress on methods of automatic coastline extraction based on remote sensing images. *Natl. Remote Sens. Bull.* **2019**, *23*, 582–602. [CrossRef]
7. Gens, R. Remote sensing of coastlines: Detection, extraction and monitoring. *Int. J. Remote Sens.* **2010**, *31*, 1819–1836. [CrossRef]
8. McFeeters, S.K. The use of the Normalized Difference Water Index (NDWI) in the delineation of open water features. *Int. J. Remote Sens.* **1996**, *17*, 1425–1432. [CrossRef]
9. Kauth, R.J.; Thomas, G. The tasselled cap–A graphic description of the spectral-temporal development of agricultural crops as seen by Landsat. In Proceedings of the LARS Symposia, West Lafayette, IN, USA, 29 June–1 July 1976; p. 159.
10. Feyisa, G.L.; Meilby, H.; Fensholt, R.; Proud, S.R. Automated Water Extraction Index: A new technique for surface water mapping using Landsat imagery. *Remote Sens. Environ.* **2014**, *140*, 23–35. [CrossRef]

11. Hossain, M.S.; Yasir, M.; Wang, P.; Ullah, S.; Jahan, M.; Hui, S.; Zhao, Z. Automatic shoreline extraction and change detection: A study on the southeast coast of Bangladesh. *Mar. Geol.* **2021**, *441*, 106628. [CrossRef]
12. Bamdadinejad, M.; Ketabdari, M.J.; Chavooshi, S.M.H. Shoreline extraction using image processing of satellite imageries. *J. Indian Soc. Remote Sens.* **2021**, *49*, 2365–2375. [CrossRef]
13. Xu, H. Modification of normalised difference water index (NDWI) to enhance open water features in remotely sensed imagery. *Int. J. Remote Sens.* **2006**, *27*, 3025–3033. [CrossRef]
14. Zollini, S.; Alicandro, M.; Cuevas-González, M.; Baiocchi, V.; Dominici, D.; Buscema, P.M. Shoreline extraction based on an active connection matrix (ACM) image enhancement strategy. *J. Mar. Sci. Eng.* **2019**, *8*, 9. [CrossRef]
15. Niculescu, S.; Bengoufa, S.; Mihoubi, M.; Belkessa, R.; Abbad, K. Rocky shoreline extraction using a deep learning model and object-based image analysis. *Remote Sens. Spat. Inf. Sci.* **2021**, *43*, 23–29. [CrossRef]
16. Fisher, A.; Flood, N.; Danaher, T. Comparing Landsat water index methods for automated water classification in eastern Australia. *Remote Sens. Environ.* **2016**, *175*, 167–182. [CrossRef]
17. Otsu, N. A threshold selection method from gray-level histograms. *IEEE Trans. Syst. Man Cybern.* **1979**, *9*, 62–66. [CrossRef]
18. Wang, E.; Hu, S.; Han, H.; Liu, C. Research on ice concentration in Heilong River based on the UAV low-altitude remote sensing and OTSU algorithm. *J. Hydraul. Eng.* **2022**, *53*, 68–77. [CrossRef]
19. Qu, L.A.; Chen, Z.; Li, M.; Zhi, J.; Wang, H. Accuracy improvements to pixel-based and object-based lulc classification with auxiliary datasets from Google Earth engine. *Remote Sens.* **2021**, *13*, 453. [CrossRef]
20. Wang, M.; Zhang, H.; Zhang, Y.; Lin, M.; Gong, P. Evolution analysis of land use pattern in the Changjiang River Delta coastal zone in recent 39 years. *Haiyang Xuebao* **2020**, *42*, 142–154. [CrossRef]
21. Hou, W.; Hou, X.; Sun, M.; Song, B. Land use/land cover change along low-middle latitude coastal areas of Eurasia and their driving forces from 2000 to 2010. *World Reg. Stud.* **2021**, *30*, 813–825. [CrossRef]
22. Breiman, L. Random forests. *Mach. Learn.* **2001**, *45*, 5–32. [CrossRef]
23. Liu, C.; Li, W.; Zhu, G.; Zhou, H.; Yan, H.; Xue, P. Land use/land cover changes and their driving factors in the Northeastern Tibetan Plateau based on Geographical Detectors and Google Earth Engine: A case study in Gannan Prefecture. *Remote Sens.* **2020**, *12*, 3139. [CrossRef]
24. Ma, Y.; Jiang, Q.; Meng, Z.; Li, Y.; Wang, D.; Liu, H. Classification of Land Use in Farming Area Based on Random Forest Algorithm. *Trans. Chin. Soc. Agric. Mach.* **2016**, *47*, 297–303. [CrossRef]
25. Zhang, H.; Qin, N.; Wang, J.; Li, M.; Yang, A.x.; Lu, Q. Spatiotemporal Pattern and Driving Factors of Land Use in Guangxi Coastal Zone. *Res. Soil Water Conserv.* **2022**, *29*, 367–374. [CrossRef]
26. Han, Y.; Zhu, J.; Wei, D.; Wang, F. Spatial-Temporal Effect of Sea–Land Gradient on Land Use Change in Coastal Zone: A Case Study of Dalian City. *Land* **2022**, *11*, 1302. [CrossRef]
27. Cui, J.; Zhu, M.; Liang, Y.; Qin, G.; Li, J.; Liu, Y. Land use/land cover change and their driving factors in the Yellow River Basin of Shandong Province based on google earth Engine from 2000 to 2020. *ISPRS Int. J. Geo-Inf.* **2022**, *11*, 163. [CrossRef]
28. Tang, S.; Song, L.; Wan, S.; Wang, Y.; Jiang, Y.; Liao, J. Long-Time-Series Evolution and Ecological Effects of Coastline Length in Coastal Zone: A Case Study of the Circum-Bohai Coastal Zone, China. *Land* **2022**, *11*, 1291. [CrossRef]
29. Nie, T.; Dong, G.; Jiang, X.; Lei, Y. Spatio-temporal changes and driving forces of vegetation coverage on the loess plateau of Northern Shaanxi. *Remote Sens.* **2021**, *13*, 613. [CrossRef]
30. Zhang, Z.; Hu, B.; Qiu, H.; Deng, Y. Spatio-temporal Differentiation and Driving Mechanism of Ecological Environment Vulnerability in Southwest Guangxi Karst-Beibu Gulf Coastal Zone. *J. Geo-Inf. Sci.* **2021**, *23*, 456–466. [CrossRef]
31. Lou, P.; Fu, B.; Lin, X.; Bi, L.; Ma, R.; Tang, T. Influence of Land Use Change on Ecosystem Service Value Based on GEE in the Beijing-Tianjin-Hebei Region from 1998 to 2018. *Environ. Sci.* **2019**, *40*, 5473–5483. [CrossRef]
32. Dong, J.; Xiao, X.; Menarguez, M.A.; Zhang, G.; Qin, Y.; Thau, D.; Biradar, C.; Moore, B., III. Mapping paddy rice planting area in northeastern Asia with Landsat 8 images, phenology-based algorithm and Google Earth Engine. *Remote Sens. Environ.* **2016**, *185*, 142–154. [CrossRef] [PubMed]
33. Xia, H.; Zhao, J.; Qin, Y.; Yang, J.; Cui, Y.; Song, H.; Ma, L.; Jin, N.; Meng, Q. Changes in water surface area during 1989–2017 in the Huai River Basin using Landsat data and Google earth engine. *Remote Sens.* **2019**, *11*, 1824. [CrossRef]
34. Yang, X.; Meng, F.; Fu, P.; Zhang, Y.; Liu, Y. Spatiotemporal change and driving factors of the Eco-Environment quality in the Yangtze River Basin from 2001 to 2019. *Ecol. Indic.* **2021**, *131*, 108214. [CrossRef]
35. Yang, X.; Meng, F.; Fu, P.; Wang, Y.; Liu, Y. Time-frequency optimization of RSEI: A case study of Yangtze River Basin. *Ecol. Indic.* **2022**, *141*, 109080. [CrossRef]
36. Dai, S.; Yi, X.; Luo, H.; Li, H.; Li, M.; Zheng, Q.; Hu, Y. Mapping Land Use in Hainan Island Based on Google Earth Engine and Landsat Time Series Data. *Chin. J. Trop. Crops* **2021**, *42*, 3351–3357. [CrossRef]
37. Yu, L.; Sun, L.; Zhang, D.; Liu, S.; Xie, Z.; Ping, X. Extraction of land-cover and wetland area in Bohai Rim region based on Google Earth Engine. *Chin. J. Appl. Ecol.* **2020**, *31*, 4091–4098. [CrossRef]
38. Jiang, T.; Wu, G.; Niu, P.; Cui, Z.; Bian, X.; Xie, Y.; Shi, H.; Xu, X.; Qu, K. Short-term changes in algal blooms and phytoplankton community after the passage of Super Typhoon Lekima in a temperate and inner sea (Bohai Sea) in China. *Ecotoxicol. Environ. Saf.* **2022**, *232*, 113223. [CrossRef] [PubMed]
39. Wei, F.; Han, G.; Han, M.; Zhang, J.; Li, Y.; Zhao, J. Temporal-spatial Dynamic Evolution and Mechanism of Shoreline and the Sea Reclamation in the Bohai Rim During 1980–2017. *Sci. Geogr. Sin.* **2019**, *39*, 997–1007. [CrossRef]

40. Sun, B.; Zuo, S.; Xie, H.; Li, H.; Yang, Z. Analysis of impact effects and changes of the coastline in the Bohai Bay during the past 40 years. *J. East China Norm. Univ.* **2017**, *4*, 139–148. [CrossRef]
41. Zhang, Y.; Liu, Y.; Zhang, X.; Huang, H.; Qin, K.; Bai, Z.; Zhou, X. Correlation Analysis between Land-Use/Cover Change and Coastal Subsidence in the Yellow River Delta, China: Reviewing the Past and Prospecting the Future. *Remote Sens.* **2021**, *13*, 4563. [CrossRef]
42. Liu, Y.; Hou, X.; Li, X.; Song, B.; Wang, C. Assessing and predicting changes in ecosystem service values based on land use/cover change in the Bohai Rim coastal zone. *Ecol. Indic.* **2020**, *111*, 106004. [CrossRef]
43. Zhang, D.-D.; Zhang, L. Land cover change in the central region of the lower Yangtze River based on Landsat imagery and the Google Earth Engine: A case study in Nanjing, China. *Sensors* **2020**, *20*, 2091. [CrossRef] [PubMed]
44. Chen, C.; Chen, H.; Liang, J.; Huang, W.; Xu, W.; Li, B.; Wang, J. Extraction of water body information from remote sensing imagery while considering greenness and wetness based on Tasseled Cap transformation. *Remote Sens.* **2022**, *14*, 3001. [CrossRef]
45. Song, Y.; Wang, Y.; Du, B.; Wang, J.; Dong, X. Detection of Overlapped Bullet Holes Based on Improved Otsu's Thresholding Method. *Acta Armamentarii* **2022**, *43*, 924. [CrossRef]
46. Wan, J.; Lin, S.; Mei, T.; Lin, Z.; Guo, T. Image Enhancement Algorithm of Electrowetting Display Based on Image Segmentation and Dynamic Histogram Equalization. *Acta Photonica Sin.* **2022**, *51*, 0210005. [CrossRef]
47. Wu, R.; Hu, X.; Mei, H.; He, J.; Yang, J. Spatial Susceptibility Assessment of Landslides Based on Random Forest: A Case Study from Hubei Section in the Three Gorges Reservoir Area. *Earth Sci. J. China Univ. Geosci.* **2021**, *46*, 321–330. [CrossRef]
48. Zhu, Y.; Zeng, Y.; Zhang, M. Extract of land use/cover information based on HJ satellites data and object-oriented classification. *Trans. Chin. Soc. Agric. Eng. (Trans. CSAE)* **2017**, *33*, 258–265. [CrossRef]
49. Wang, N.; Li, Q.; Du, X.; Zhang, Y.; Zhao, L.; Wang, H. Identification of main crops based on the univariate feature selection in Subei. *Natl. Remote Sens. Bull.* **2017**, *21*, 519–530. [CrossRef]
50. Pan, L.; Xia, H.; Yang, J.; Niu, W.; Wang, R.; Song, H.; Guo, Y.; Qin, Y. Mapping cropping intensity in Huaihe basin using phenology algorithm, all Sentinel-2 and Landsat images in Google Earth Engine. *Int. J. Appl. Earth Obs. Geoinf.* **2021**, *102*, 102376. [CrossRef]
51. Zhuang, D.; Liu, J. Study on the model of regional differentiation of land use degree in China. *J. Nat. Resour.* **1997**, *12*, 105–111.
52. Liu, H.; Zheng, M.; Liu, J.; Zheng, X. Sustainable land use in the trans-provincial marginal areas in China. *Resour. Conserv. Recycl.* **2020**, *157*, 104783. [CrossRef]
53. Wang, J.; Xu, C. Geodetector: Principle and prospective. *Acta Geogr. Sin.* **2017**, *72*, 116–134. [CrossRef]
54. Xu, J.; Liu, S.; Zhao, S.; Wu, X.; Hou, X.; An, Y.; Shen, Z. Spatiotemporal dynamics of water yield service and its response to urbanisation in the Beiyun river Basin, Beijing. *Sustainability* **2019**, *11*, 4361. [CrossRef]
55. Hou, X.; Zhang, H.; Li, D.; Hou, W.; Song, Y. Development trend, environmental and ecological impacts, and policy recommendations for Bohai Sea reclamation. *Acta Ecol. Sin.* **2018**, *38*, 3311–3319. [CrossRef]